Highly Ordered Mesoporous Carbon Synthesized via in Situ Template for Supercapacitors

Ding Sheng Yuan[*], *Jianghua Zeng, Jingxing Chen, Yingliang Liu*

Department of Chemistry, Jinan University, Guangzhou 510632, China
[*]E-mail: tydsh@jnu.edu.cn

An in-situ silica template method has been employed to prepare mesoporous carbon materials. As-prepared carbon materials have been characterized by transmission electron microscopy, small-angle X-ray diffraction, N_2 adsorption-desorption, Fourier transform infrared spectroscopy and electrochemical techniques. The results reveal that highly ordered mesoporous carbon with abundant hydrophilic functional groups and high specific surface area (1628 m^2 g^{-1}) was obtained. Such material has high specific capacitance (161 F g^{-1}) and the capacitance shows negligible dependence on the potential sweep rate, which makes it promising in supercapacitor application.

1. INTRODUCTION

Electrochemical double layer capacitor (EDLC) has attracted considerable attention because of its wide potential applications in electric vehicles and other high power applications due to its high power density and long cycle life [1-3]. So far activated carbons are mostly investigated and have been commercially applied to EDLCs. However, their essential micropores are too small to be fully accessible by electrolytes in the charge/discharge process and the exposed surface in micropores is not to be efficiently utilized for charge storage at high loading current density [4-6]. It is believed that carbons with a porosity formed almost exclusively by mesopores could be potentially more advantageous as EDLCs electrodes than activated carbons. Recently, highly ordered mesoporous carbons (HOMCs) have attracted broad interest because of their well-defined structure and appropriately pore size and high specific surface area [7-13]. A hard-template based method has been normally used to synthesize these materials. This is achieved by the filling of the pores from the ordered mesoporous silica materials (such as SBA-15, MCM-41 and MCM-48) with a carbon

precursor, subsequent carbonization of the composite and final removal of the inorganic template. For example, Hyeon's group first reported the synthesis of self-ordered mesoporous carbon using the ordered mesoporous silica MCM-48 as the template and phenol-formaldehyde resin as the carbon source [1]. However, most of these methods involve the tedious preparation of mesoporous silica hard template in advance, which limits their practical large scale fabrication.

Here, we report on the one-step synthesis of HOMC via an in-situ synthesized silica template route using diluted sulfuric acid (8 wt%) as cross-linked reagent and P123 ($EO_{20}PO_{70}EO_{20}$，Ma=5800) and sucrose as the carbon precursors. Small-angle X-ray diffraction (SA-XRD) and high-resolution transmission electron microscopy (HRTEM) and N_2 adsorption-desorption analysis confirms the synthesized material is highly ordered and possesses well-defined mesoporous structure with 4 nm pore size. HOMCs as electrode materials for EDLCs exhibit high specific capacitance and this specific capacitance does not decay with the increase of potential sweep rate, as opposed to the many other forms of carbons, which usually show significant reductions.

2. EXPERIMENTAL PART

2.1. Direct synthesis of HOMCs

All the chemical reagents in this work were of analytical grade purity. HOMCs were synthesized from silica/P123/sucrose according to a reported procedure [7, 8] with some modifications. A detailed procedure is as follows: (1) 5−10 g P123 was dissolved in 8 wt% sulfuric acid (150 mL) under vigorously stirring at 35−40 ^{o}C. Then 20 g tetraethyl orthosilicate (TEOS) was dropped into the solution and stirred for 24 h. The resultant solution was aged at 100 ^{o}C for 48 h. to give the silica/P123/sucrose composite. (2) The composite was dried at 100−160 ^{o}C for 6 h and carbonized under N_2 atmosphere at 850−950 ^{o}C for 2 h. (3) HOMCs were obtained by treatment in 15 wt% HF solution for 24 h to remove the silica template.

2.2 Characterization of HOMCs

The morphology of the HOMCs was examined using a transmission electron microscope (JEOL HRTEM-2010, 200 kV). The SA-XRD pattern was obtained on a Rigaku D/max-2500 X-ray diffractometer (XRD, Cu Kα, 40kV, 20mA, λ =1.5406Å). The specific surface areas were measured via the Micromertics TriStar 3000 Analyzer. The functional groups on the surface of HOMCs were detected via Nicolet 6700 FT-IR spectrometer.

2.3 Electrochemical measurements

The working electrode was prepared by pressing the mixture of HOMCs and carbon black and 5%-PTFE (80:10:10 wt%) into a 12×16 mm foam nickel electrode under 35 MPa. The scheme for the electrode preparation and the practical electrodes are presented in Fig.1.
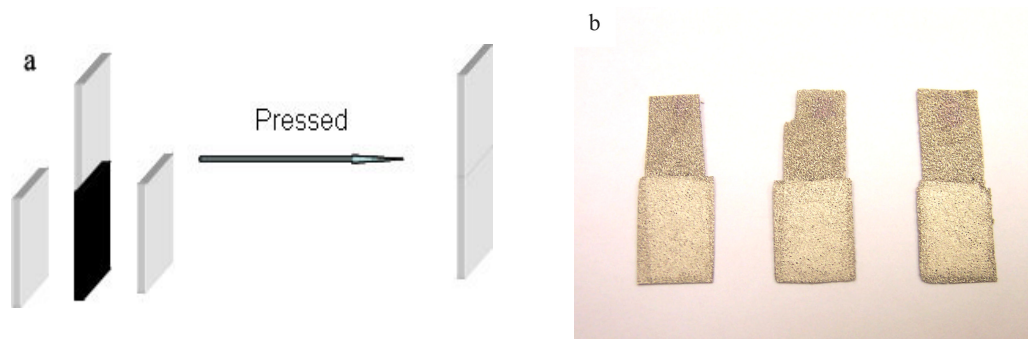
Figure 1. (a) Scheme for the electrode preparation and (b) Pictures of the working electrodes.

All electrochemical measurements were conducted on a Princeton EC-Lab VMP2 electrochemical workstation. The experiments were carried out in a standard three electrodes cell containing a nickel foil electrode as a counter and an Hg/HgO (6.0 mol L^{-1} KOH) as a reference electrode and the above-mentioned working electrode. An aqueous solution containing 6 mol L^{-1} NaOH was used as electrolyte solution. Different sweep rates (1, 5, 20, 50 and 100 mV s^{-1}) were employed in cyclic voltammetry within the range of -0.9−0.1 V vs Hg/HgO. Electrochemical impedance spectroscopy (EIS) was carried out at -0.400 V vs Hg/HgO at the frequency range of 5 mHz ~10 kHz and the amplitude of 5 mV.
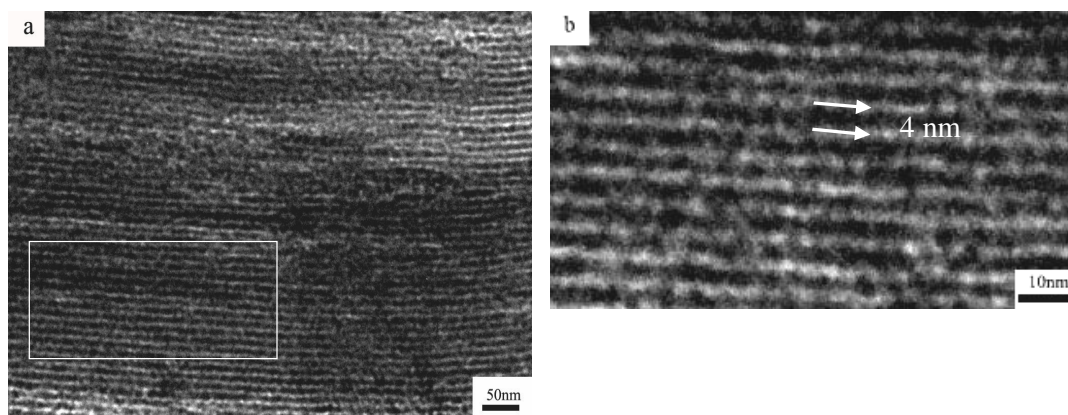

Figure 2. (a) TEM image and (b) HRTEM image of as-prepared sample.

3. RESULTS AND DISCUSSION

The mesoporous carbon with the different pore sizes of 2.2−8.1 nm were synthesized using P123 and glucose as carbon sources via in-situ silica template. We have investigated various factors affecting the preparation of HOMC and an optimized synthesis condition was identified to include the drying process at 160 ^{o}C for 6 h and the carbonization at 850 ^{o}C for 2h and heating rate of 1 ^{o}C min^{-1}. Fig. 2 shows the TEM images of a typical sample synthesized under the optimum synthesis condition

and aged in open vessel (denoted as HOMC-1). It can be seen that 2-D highly ordered MC is obtained. The magnified TEM image (Fig. 2b) illustrates that the size of pores is approximately 4 nm.

To further reveal the mesoporous structure of HOMCs, the SA-XRD analysis was carried out on HOMC-1(Fig. 3a). The obtained diffraction pattern presents certain degree of periodic order with a strong intensity from both (110) and (200) planes. The visible high index peak (200) indicates a high periodic order in the arrangement of symmetry cells in agreement with the TEM observations. This result is consistent with Wang and co-workers' report [14].
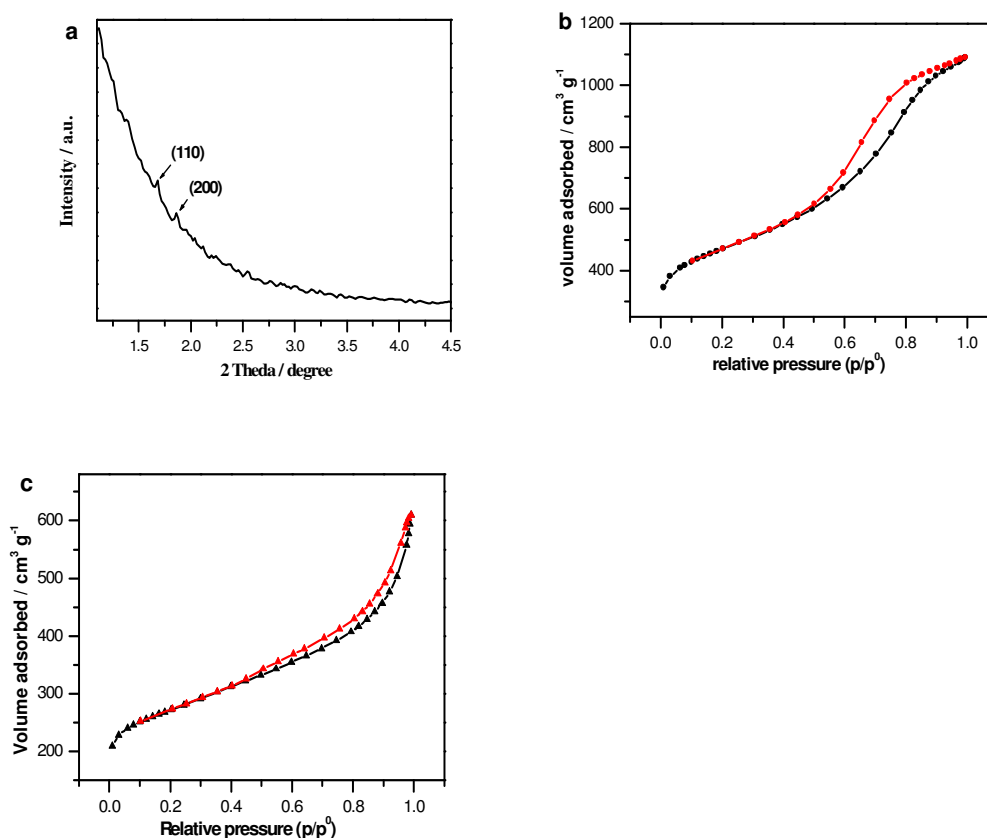

Figure 3. (a) SAXRD pattern of HOMCs and N_2 adsorption-desorption isotherms of (b) HOMC-1 and (c) HOMC-2.

The pore structure and surface area of HOMCs was investigated by N_2 adsorption-desorption method. Fig. 3b and 3c show the obtained N_2 adsorption-desorption isotherms for HOMC-1 and another sample obtained under optimum condition and aged in a closed vessel (denoted as HOMC-2). A type IV isotherm with a sharp capillary condensation step at high relative pressures is observed for both samples and a hysteresis loop near relative pressure of 0.60 in the desorption branch indicates the presence of mesopores. The measured results then reveal that HOMCs contain abundant mesopores. Their pore size distributions calculated from the absorption branches by the Barrentt-Joyner-Halenda method are centered at 3.7 nm and 4.1 nm, respectively. Surprisingly, the measured BET area of HOMC-1 differs greatly from HOMC-2 (1628 vs 935 m^2 g^{-1}). The exact reason for the property

difference is not clear yet. It is probably related to the water content difference, as a lot of water will evaporate during aging in an open vessel.

The functional groups of HOMCs were characterized by FT-IR, as shown in Fig. 4. The strong characteristic peak at 3437 cm^{-1} is attributed to the stretching vibration of O–H bond and the small peaks at 2914 and 2841 cm^{-1} are originated from the stretching vibration of C–H bond. The peak at 1379 cm^{-1} corresponds to the stretching vibration of C-O bond. The infrared spectra peaks at 1702 cm^{-1} and 1623 cm^{-1} are due to the stretching vibration of carboxyl groups C=O and C=C bond [15]. FT-IR spectrum confirms that there are many functional groups distributed at the surface of the HOMCs.
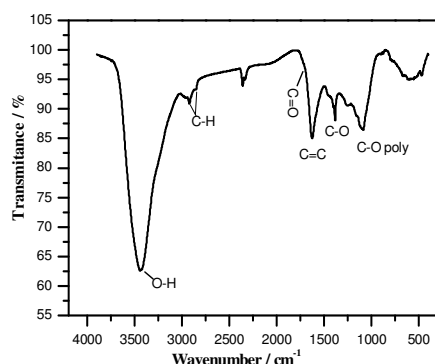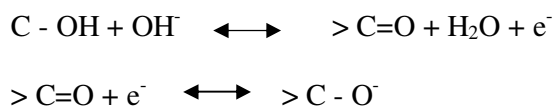

Figure 4. FT-IR spectrum of the HOMC.

These functional groups improve the hydrophilicity and wettability of HOMCs and it is advantageous to the aqueous supercapacitor. The functional groups will contribute to the pseudocapacitance via the redox reactions during the charge-discharge process [13, 16].

$$C - OH + OH^- \longleftrightarrow\ >C=O + H_2O + e^-$$

$$>C=O + e^- \longleftrightarrow\ >C - O^-$$

HOMCs could be a good candidate as electrode material for the electrochemical capacitors owing to their ordered mesoporous structure and high BET surface area. Here cyclic voltammetry is used to study double-layer capacitor materials and resulting EDLC devices, as it provides detailed information directly on the double-layer capacitance and its potential dependence, which is essential for examining the behaviour and structure of electrified interfaces [12]. As shown in Fig. 5a, HOMC-1 shows slightly higher capacitance than HOMC-2, which may be explained by the higher surface area of the former, since both the double layer capacitance and pseudocapacitance are interfacial phenomena. The slopes of current variation near the vertex potentials are vertical at 5 mV s^{-1}, indicating the excellent behavior of HOMCs as electrode materials [17]. An ideal behavior of an EDLC should exhibit a rectangular shape on the voltammogram. The deviation from this rectangular shape is due to the presence of functional groups on the HOMC surface as supported by the FT-IR

experiment, which may lead to redox reactions. The electrochemical performance of HOMCs is similar to the results of nitrogen-enriched carbon reported by Hulicova et al. [18] and MCs synthesized by Hyeon's group [5]. As shown in Fig.5b and 5c, different as the sweep rates are, CVs of HOMCs retain a similar shape even at high sweep rate, indicating that HOMCs possess high conductivity. In the meantime, a closer look at Fig. 5b and 5c tells that HOMC-2 are better than HOMC-1, as evidenced by the still vertical slope of the current near vertex potential at high sweep rate. These results indicate the unrestricted motion of electrolytes in the pores of HOMC-2 during the double-layer formation and also reflect that the ohmic resistance for electrolyte motion in carbon mesopores is small.
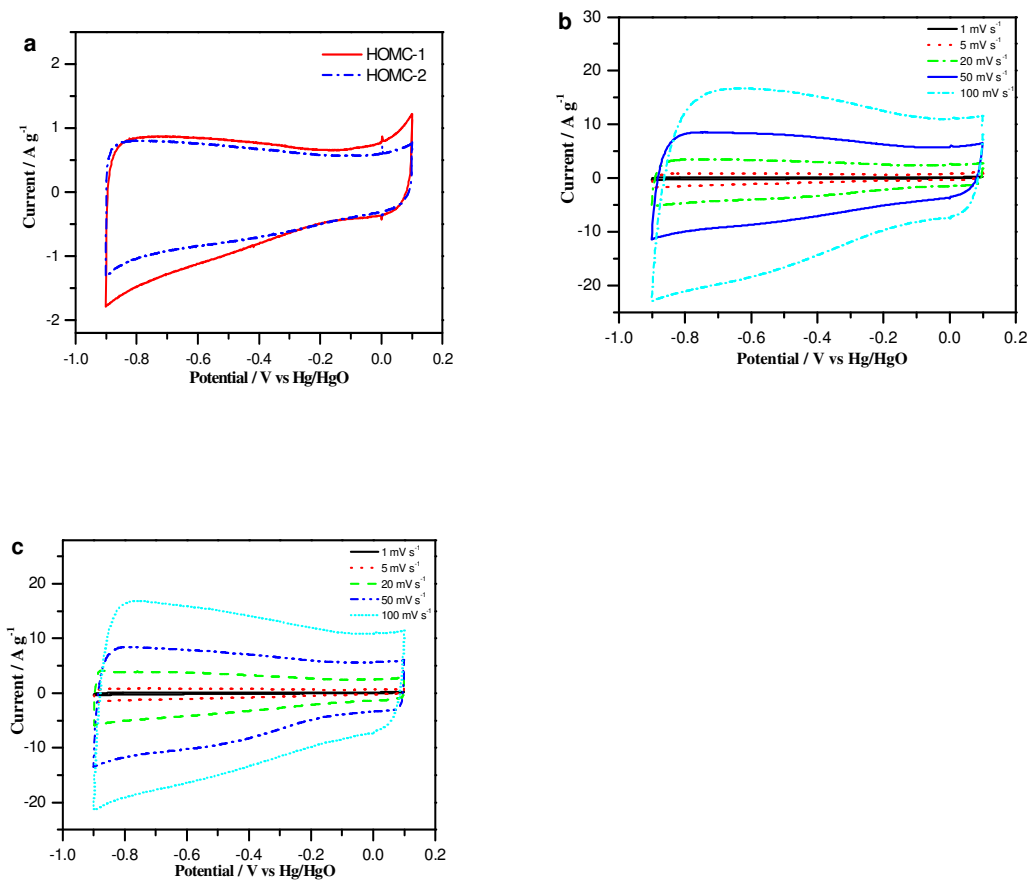

Figure 5. (a) CVs of HOMCs in 6 mol L^{-1} KOH at room temperature and sweep rate of 5 mV s^{-1}. (b and c) CVs of HOMC-1 and HOMC-2 at different sweep rates.

The gravimetric specific capacitance (*C*) of electrode is calculated according to the following Eq. (1) from charge-discharge measurement of CVs:

$$C = \frac{Q}{WV} = \frac{\int i\,dt}{W\Delta V} \qquad (1)$$

where *i, W* and ΔV are the sample current and the weight of active materials and the total potential deviation of the voltage window, respectively. The data calculated from CVs of HOMCs are listed in Table 1. A maximum gravimetric specific capacitance of 161 F g^{-1} is obtained for HOMC-1 at the sweep rate of 5 mV s^{-1}, in agreement with its large BET surface area. Usually, the specific capacitance of carbon materials decreases with increase of sweep rate, due to the increase of the resistance of ion migration in the pores [14, 19]. In this study, however, we find that the specific capacitance of HOMCs varies little in the range from 1 to 100 mV s^{-1}. Especially for HOMC-2, there is essentially no decay in the specific capacitance at all. This illustrates the unrestricted motion of electrolytes in the ~4 nm mesopores even under high sweep rate, which makes this material very promising for capacitor application.

Table 1. The specific capacitances calculated from cyclic voltammetry at the HOMC electrodes for aqueous electrolyte of 6 mol L^{-1} KOH

Electrode	Sweep rate (mV s^{-1})	Gravimetric *C* (F g^{-1})	Area-normalized *C* (μF cm^{-2})	Volumetric *C* (F cm^{-3})
HOMC-1	1	134	8.2	81
	5	161	9.9	97
	20	150	9.2	90
	50	136	8.4	82
	100	133	8.2	80
HOMC-2	1	105	11.2	121
	5	133	14.2	153
	20	138	14.8	159
	50	144	15.4	166
	100	130	13.9	151

To further investigate the influence of ordered mesoporous structure on ion diffusion, EIS has been conducted on HOMCs, as it is able to distinguish the actual electrochemical diffusion process, from the resistance and capacitance within the mesoporous carbon materials [14, 20, 21].

EIS response to a capacitive porous carbon material usually involves three processes [20]: (1) at high-frequency region, mass transfer can be neglected, so charge transfer at the electrode interface will be dominant; (2) at medium-frequency region, the dominant process would be ion diffusion in mesoporous channels, which contributes the most to the development of capacitive behavior[14]; and (3) at low-frequency region, non-homogeneous diffusion in the less-accessible sites or leakage current may govern the impedance. Nyquist plots for HOMC-1 and HOMC-2 are presented in Fig. 6a. The impedance plots exhibit two distinct parts including a semicircle in the high frequency region and a sloped line in the low frequency region. The charge transfer resistance can be estimated from the semicircle diameter of the high-frequency loop and the electrolyte ion diffusion into mesopore is characterized by the linear part of the sloped line. A pure capacitor should exhibit a vertical line at low frequency. The deviation from the vertical line is attributable to the inner-mesopore diffusion

resistance for electrolyte ions, which is strongly dependent on the detailed mesoporous structure of the different samples [14]. The smaller semicircle and bigger slope of HOMC-2 indicate its lower charge transfer resistance on electrode/electrolyte interface and its better capacitive behavior. On the other hand, the knee frequency is considered to be the critical frequency where EDLC begins to exhibit capacitive behavior. The knee frequencies for HOMC-1 and HOMC-2 are 408 and 500 Hz, respectively, implying the formation of capacitance in HOMC-2 at relatively high frequency. In the phase angle plot, the approaching to a more capacitive behavior at low frequency is usually identified with the phase angle approaching to the negative 90 degree [21, 22]. Therefore, the value of the phase angle is used to evaluate the effectiveness of ion diffusion in mesopores. That is, the smaller the phase angle, the better the capacitive performance and the faster the ions diffusion [14]. Bode plot in Fig. 6b also clarifies that HOMC-2 possesses faster ion diffusion, which is consistent with the analysis by CV. At this moment, we are still not clear why the aging at open and close conditions will render different properties, which will be the focus of our future work.
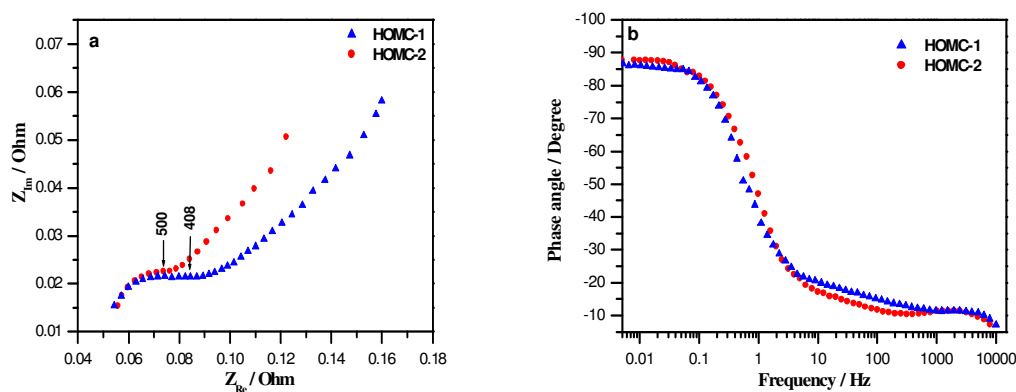

Figure 6. EIS analysis of HOMCs. (a) Nyquist plot, (b)Bode plot.

4. CONCLUSIONS

HOMCs have been synthesized via the in-situ silica template technique using glucose and P123 as the carbon sources. HOMCs with high specific surface area and abundant hydrophilic functional groups have been used as the electrode materials in EDLCs. Electrochemical measurements indicate that HOMC aged in the open vessel exhibits high surface area (1628 m^2 g^{-1}) and high specific capacitance (161 F g^{-1}) at low sweep rate of 5 mV s^{-1}. Although the value is slightly lower, the specific capacitance of HOMC aged in the closed vessel does not decay in the range from 1 to 100 mV s^{-1}, demonstrating its capability of fast ion diffusion within its mesoporous structure. The excellent performance makes HOMCs as potential candidate for electrode materials in EDLCs.

References

1. J. Lee, S. Yoon, T. Hyeon, S.M. Oh and K.B. Kim, *Chem. Commun.*, 21(1999) 2177
2. I. Moriguchi, Y. Koga, R. Matsukura, Y. Teraoka and M. Kodama, *Chem. Commun.*, 24(2002) 1844
3. J. Lee, S. Yoon, S.M. Oh, C.H. Shin and T. Hyeon, *Adv. Mater.*, 12 (2000) 359
4. D.S. Yuan, J.X. Chen, X.C Hu, J.H. Zeng, S.X. Tan and Y.L. Liu, *Int. J. Electrochem. Sci.,* 3(2008)1268
5. J. Lee, J. Kim, Y. Lee, S. Yoon, S.M. Oh and T. Hyeon, *Chem. Mater.*, 16 (2004) 3323
6. H.Y. Liu, K.P. Wang and H.S. Teng, *Carbon*, 43 (2005) 559
7. L.X. Li, H.H. Song and X.H. Chen. *Micropor. Mesopor. Mater.,* 94 (2006) 9
8. J. Kim, J. Lee and T. Hyeon. *Carbon*, 42 (2004) 2711
9. A.G. Pandolfo and A. F. Hollenkamp, *J. Power Sources*, 157 (2006) 11
10. B.E. Conway, Electrochemical Supercapacitors Scientific Fundamentals and Technological Application. New York: Kluwer/Plenum; 1999
11. M. Lazzari, F. Soavi and M. Mastragostino, *J. Power Sources*, 78 (2008) 490
12. J.J. Niu, W.G. Pell and B.E. Conway, *J. Power Sources*, 56 (2006) 725
13. E. Frackowiak, K. Metenier, V. Bertagna and F. Beguin, *Appl. Phys. Lett.*, 77 (2000) 2421
14. D.W. Wang, F. Li, H.T. Fang, M. Liu, G. Q. Lu and H.M. Cheng, *J. Phys. Chem*. B, 110 (2006) 8570
15. C.H. Cheng, J. Lehmann, J.E. Thies, S.D. Burton and M.H. Engelhard, *Organic Geochem.*, 37 (2006) 1477
16. S.W. Hwang and S.H. Hyun, *J. Non-Cryst. Solids,* 347 (2004) 238
17. J.H. Kim, Y.S. Lee, A. K. Sharma and C.G. Liu, *Electrochim. Acta.*, 52 (2006) 1727
18. D. Hulicova, M. Kodama and H. Hatori, *Chem. Mater.*, 16 (2006)2318
19. D.S. Yuan, J.X. Chen, J.H. Zeng and S.X. Tan, *Electrochem. Commun.*, 10 (2008) 1067
20. W. Sugimoto, H. Iwata, K. Yokoshima, Y. Murakami and Y. Takasu, *J. Phys. Chem*. B, 109 (2005) 7330
21. E. Barsoukov, J.R. Macdonald, Impedance Spectroscopy: Theory Experiment and Applications. New York: John Wiley & Sons, 2005
22. K. Honda, T.N. Rao, D.A. Tryk, A. Fujishima, M. Watanabe, K. Yasui and H. Masuda, *J. Electrochem. Soc.*, 148 (2001) A668